Neuro-Oncology

Neuro-Oncology 17(11), 1474–1485, 2015
doi:10.1093/neuonc/nov042
Advance Access date 29 March 2015

The metalloprotease-disintegrin ADAM8 contributes to temozolomide chemoresistance and enhanced invasiveness of human glioblastoma cells

Fangyong Dong†, Michael Eibach†, Jörg W. Bartsch†, Amalia M. Dolga, Uwe Schlomann, Catharina Conrad, Susanne Schieber, Oliver Schilling, Martin L. Biniossek, Carsten Culmsee, Herwig Strik, Garrit Koller, Barbara Carl, and Christopher Nimsky

Department of Neurosurgery, Philipps-University Marburg, Marburg, Germany (F.D., M.E., J.W.B., U.S., C.Co., S.S., B.C., C.N.); Department of Neurosurgery, Tongji Hospital, Wuhan, China (F.D.); Philipps-University Marburg, Institute for Pharmacology and Clinical Pharmacy, Marburg, Germany (A.M.D., C.Cu.); Institute of Molecular Medicine and Cell Research, University of Freiburg, Freiburg, Germany (O.S., M.L.B.); BIOSS Centre for Biological Signaling Studies, University of Freiburg, Freiburg, Germany (O.S.); Department of Neurology, Philipps-University Marburg, Marburg, Germany (H.S.); Biomaterials, Biomimetics and Biophotonics Research Group, King's College London Dental Institute, London, United Kingdom (G.K.)

Corresponding Author: Jörg W. Bartsch, PhD, Philipps-University Marburg, Laboratory, Department of Neurosurgery, University Hospital Marburg, Baldingerstr., 35033 Marburg (jbartsch@med.uni-marburg.de).

†These authors contributed equally to this work.

Background. Despite multimodal treatment, glioblastoma (GBM) therapy with temozolomide (TMZ) remains inefficient due to chemoresistance. Matrix metalloproteinase (MMP) and a disintegrin and metalloprotease (ADAM), increased in GBM, could contribute to chemoresistance and TMZ-induced recurrence of glioblastoma.

Methods. TMZ inducibility of metalloproteases was determined in GBM cell lines, primary GBM cells, and tissues from GBM and recurrent GBM. TMZ sensitivity and invasiveness of GBM cells were assessed in the presence of the metalloprotease inhibitors batimastat (BB-94) and marimastat (BB-2516). Metalloprotease-dependent effects of TMZ on mitochondria and pAkt/phosphatidylinositol-3 kinase (PI3K) and phosphorylated extracellular signal-regulated kinase 1/2 (pERK1/2) pathways were analyzed by fluorescence activated cell sorting, morphometry, and immunoblotting. Invasiveness of GBM cells was determined by Matrigel invasion assays. Potential metalloprotease substrates were identified by proteomics and tested for invasion using blocking antibodies.

Results. TMZ induces expression of MMP-1, -9, -14, and ADAM8 in GBM cells and in recurrent GBM tissues. BB-94, but not BB-2516 (ADAM8-sparing) increased TMZ sensitivity of TMZ-resistant and -nonresistant GBM cells with different O^6-methylguanine-DNA methyltransferase states, suggesting that ADAM8 mediates chemoresistance, which was confirmed by ADAM8 knockdown, ADAM8 overexpression, or pharmacological inhibition of ADAM8. Levels of pAkt and pERK1/2 were increased in GBM cells and correlated with ADAM8 expression, cell survival, and invasiveness. Soluble hepatocyte growth factor (HGF) R/c-met and CD44 were identified as metalloprotease substrates in TMZ-treated GBM cells. Blocking of HGF R/c-met prevented TMZ-induced invasiveness.

Conclusions. ADAM8 causes TMZ resistance in GBM cells by enhancing pAkt/PI3K, pERK1/2, and cleavage of CD44 and HGF R/c-met. Specific ADAM8 inhibition can optimize TMZ chemotherapy of GBM in order to prevent formation of recurrent GBM in patients.

Keywords: chemoresistance, glioblastoma, hydroxamate inhibitors, metalloproteases, TMZ.

Glioblastoma (GBM) is the most common malignant primary neoplasm of the brain in adults. Despite multimodal treatment encompassing surgical resection, chemotherapy, and radiotherapy, prognosis remains infaust with a mean survival of <15 months.[1] The key biological features of GBM are unlimited tumor cell proliferation, widespread infiltrative growth, and angiogenesis.[2] Temozolomide (TMZ) combined with surgical resection and radiotherapy is the standard regimen for malignant glioma[3,4]; however, acquired chemoresistance of glioma cells, in particular in highly invasive glioma

Received 13 December 2013; accepted 22 February 2015

cells, limits its efficacy. TMZ exerts its cytotoxic effect via alkylation of the O^6 position of guanine,[5,6] thereby inducing DNA damage response.[7,8]

TMZ resistance mechanisms range from (i) remodeling of the electron transport chain with significant increased activity of mitochondrial complexes II/III and cytochrome C oxidase to (ii) DNA repair protein O^6-methylguanine-DNA methyltransferase[9] (MGMT), sonic hedgehog, and Notch pathways.[10] Notably, ectodomain cleavage of membrane proteins dependent on matrix metalloproteinase (MMP) and a disintegrin and metalloprotease (ADAM) can regulate DNA damage response and radiosensitivity of glioblastoma stem cells.[11,12] MMPs and ADAM proteases constitute 2 families of zinc-dependent endopeptidases.[13] Numerous studies have confirmed the role of MMPs in tumor cell invasion[14] and angiogenesis.[15]

In malignant glioma, elevated expression levels of MMP-1, -2, -7, -9, -11, -12, -14, and -19 have been reported, and for some MMPs there is a correlation between their expression and tumor progression in vivo.[16–19] MMP-9, MMP-2, and its activator MMP-14 have been demonstrated to contribute to active migration and invasion of tumor cells into surrounding brain tissue.[20,21] MMP-2 inhibition in glioma cell lines decreased radiation-induced MMP-2 expression, cell viability, and radiation-enhanced migration and invasion.[22] Based on these results, a combined therapy regimen of TMZ plus marimastat was tested in clinical phase II trials with limited success, suggesting the presence of effector metalloproteases (MPs) spared by marimastat[23] that could be members of the ADAM protease family.

As type I transmembrane proteins, 21 ADAM members are found functional in humans[24,25] with important roles in cell adhesion, invasion, and cell signaling.[13,26,27] Similar to MMPs, mounting evidence indicates that ADAM proteins regulate tumorigenesis, invasiveness, and proliferation.[27,28] For instance, the L1 cell adhesion molecule (L1CAM) (cluster of differentiation [CD]171), a transmembrane protein involved in growth and invasion, is cleaved by ADAM10 and presenilin, resulting in an L1 intracellular domain that is translocated to the cell nucleus, thereby regulating gene expression, DNA damage response, and radiosensitivity of glioblastoma stem cells.[11,12] In addition, hyaluronic acid receptor (CD44) and the hepatocyte growth factor receptor (HGF R/c-met) were shown to be essential[29,30] for glioma invasion. Both proteins are described in the context of chemoresistance of glioma cells[31,32] and are regulated by shedding via MMPs and/or ADAM proteases. Compared with nonneoplastic brain tissue, expression levels of ADAM8 and ADAM17 in glioblastoma are significantly increased and correlate with the malignant phenotypes, respectively.[28,33,34] In a recent study, ADAM8 was shown to confer chemoresistance to cisplatin in A549 lung cancer cells.[35] Here we investigated the contribution of MMPs and ADAMs on TMZ chemoresistance of GBM cells in general and defined ADAM8 as an important target molecule.

Materials and Methods

Cell Lines and Tumor Tissue Samples

Established U87 and U251 glioblastoma cell lines were purchased from the American Type Culture Collection and kindly provided by Dr M. Ocker. Collection and processing of primary human GBM tumor samples was in accordance with the ethical standards of the 2008 Helsinki Declaration. Informed consent of patients was obtained for acquisition, processing, and documentation of pseudonymized samples as approved by the local ethics committee (Medical Faculty, Marburg University). GBM29, GBM42, and GBM98 cells were prepared from World Health Organization (WHO) grade IV GBM specimens collected directly after surgery as described (see Supplementary material, Methods). MGMT status of all GBM cells was determined using a methylation-specific PCR (ZymoResearch). Whereas U87, U251, and GBM29 are methylated, primary GBM cells GBM42 and GBM98 have an unmethylated MGMT promoter status.

Antibodies and Inhibitors

Antibodies directed against Akt (panAkt and pAkt S473), cytochrome C oxidase IV, and extracellular signal-regulated kinase (ERK)1/2 (panERK and pERK1/2 Tyr 202/204) were obtained from Cell Signaling; β-tubulin from Santa Cruz Biotechnology; MMP-14 from Epitomics, and ADAM8 from R&D Systems. As blocking antibodies, we used a control immunoglobulin G (IgG), an anti-CD44 (Hermes-1, MA4400, Thermo Scientific), and an anti-HGF R/c-met (R&D Systems). As an ERK1/2 inhibitor, we used U0126 (Cell Signaling); as an Akt/PI3K inhibitor, LY294002 (Cell Signaling); and as a specific ADAM8 inhibitor, BK-1361[36] (Peptide 2.0).

Media and Solutions for Cell Culture

GBM cell lines were cultured in Dulbecco's modified Eagle's medium (DMEM) high glucose (4.5 g/L) supplemented with 1% L-glutamine (200 mM), 1% penicillin/streptomycin, 1 mM sodium pyruvate solution, 1% Minimum Essential Medium Eagle nonessential amino acids, and 10% fetal bovine serum (heat inactivated). For activity and proteomic analysis, growth medium was exchanged with DMEM high glucose (4.5 g/L) without fetal bovine serum and phenol red 24 h before collecting the supernatants. All materials above were bought from PAA Laboratories.

Real-time Quantitative Polymerase Chain Reaction

Real-time quantitative PCR (qPCR; ABI StepOnePlus) was performed as described by Primer Design. For experimental details, see Supplementary material, Methods. Relative changes in gene expression were determined with the delta cycle threshold (ΔCt) method using the formula: $\Delta Ct = (Ct\ \text{reference} - Ct\ \text{target})$. Differential gene expression between conditions corresponds to the $\log_2$ fold-difference in mRNA levels between conditions compared.[37]

Analysis of Cell Viability

Cells were seeded onto 8-well chambers (Sarstedt). After indicated incubation times, cells were fixed with 4% paraformaldehyde and stained with Hoechst dye. Numbers of surviving cells were counted in 50 independent viewing fields in triplicates.

Preparation of Lysates

Cell culture medium was aspirated and we added radioimmunoprecipitation assay buffer (50 mM HEPES [4-(2-hydroxyethyl)-1-piperazine ethanesulfonic acid], pH 7.4, 150 mM NaCl, 1% NP-40 [nonyl phenoxypolyethoxylethanol], 0.5% Na-desoxycholate, 0.1% sodium dodecyl sulfate [SDS], 10 mM phenanthroline/EDTA, protease inhibitor cocktail "complete," 600 μL/dish), followed by incubation at 4°C for 15 min. Cell scrapers were used to collect the lysates. The samples were sonicated and centrifuged at 13 000 rpm for 5 min to remove cell debris. Protein concentrations were determined using bicinchoninic acid (Thermo Scientific) as per manufacturer's instructions.

Zymography Assays

Protein samples were prepared in nonreducing sample buffer (125 mM Tris-HCl, pH 6.8, 20% glycerol, 4% SDS, 0.005% bromophenol blue) without boiling. Substrates (either gelatin or casein, 0.1%) were added in a separating gel to copolymerize with polyacrylamide. During electrophoresis, proteins were separated while SDS present in the gel preserved MMPs in an inactive state. After electrophoresis, gels were washed with renaturing buffer (2.5% Triton-X100; 2 × 30 min each), resulting in partially renatured MMPs with restored activity. The gel was incubated in developing buffer (50 mM Tris, pH 7.5, 200 mM NaCl, 4 mM $CaCl_2$, and 0.02% Brij-35; 30 min at room temperature, followed by 24 h at 37°C in fresh developing buffer). Next day, the gel was dyed in Coomassie staining buffer for 1 h followed by Coomassie destaining solution to visualize bands of active enzymes.

Western Blot

Whole cell lysates were prepared in 5 × loading buffer (0.2 M Tris-HCl, pH 6.8, 20% glycerol, 10% SDS, 10 mM β-mercaptoethanol). Samples were denatured at 95°C for 10 min, and after electrophoresis, separated proteins were transferred onto nitrocellulose membranes. Detection of target proteins was performed using specific antibodies. For detection, horseradish peroxidase (HRP)–conjugated antibodies were diluted 1:2000 (anti-goat HRP and anti-rabbit HRP; Abcam) in conjunction with chemiluminescent substrate (Super Signal West Pico, Thermo Scientific). Chemiluminescence was determined using a Chemostar Imager (Intas).

Protease Activity Assays

Synthetic fluorescence resonance energy transfer peptides were used to monitor protease activities of MMP-14 and ADAM8 in cell supernatants as described.[28] For experimental details, see Supplementary material, Methods.

Invasion Assays

Inserts (8.0 μM pore size, BD Falcon) were transferred into 24-well plates. Each insert was loaded with 75 μL Matrigel (BD Biosciences), 1:3 diluted with phosphate buffered saline. Cell suspension was prepared in serum-free DMEM containing 5000 cells/300 μL/invasion chamber. For function blocking of CD44 and HGF R/c-met, antibodies (10 mg/mL) were preincubated with the cells 1 h prior to application. Complete DMEM (750 μL) was added into each lower chamber as chemoattractant and incubated at 37°C 5% CO_2 for 24 h. A cotton swab was used to remove noninvading cells. Invaded cells on the lower surface were fixed with 4% paraformaldehyde for 15 min, stained with hematoxylin solution at room temperature for 5 min, washed with ddH_2O (3 × 10 min), and counted by microscopy. Experiments were repeated 3 times, counting 10 random viewing fields per well respectively.

Quantitative Proteomic Analysis of Cell Conditioned Medium

To generate cell conditioned medium (CCM), U87 cells were kept for 24 h in serum-free DMEM high glucose (4.5 g/L) with 700 μM TMZ. Cells were treated with 100 nM BB-94 or the corresponding solvent control. Quantitative proteomic analysis of CCM was performed as described previously[38] using isotopic formaldehyde labeling, cation exchange chromatography prefractionation, and a QSTAR Elite (Applied Biosystems) mass spectrometer for liquid chromatography–tandem mass spectrometry analysis. Data analysis was performed as described.[38] Log_2 transformed ratios are expressed as BB-94 treatment/control.

ELISA Assays

Supernatants were collected after incubation of U87 cells with indicated concentrations of TMZ for 5 days. After normalization for protein concentrations, cell supernatants were subjected to ELISA assays to detect soluble met (c-met soluble Human ELISA Kit, Life Technologies) and CD44 (CD44 Human ELISA Kit, Abcam). ELISAs were performed according to the manufacturer's' instructions. For calibration curves using standard concentrations, linear regression analysis resulted in a coefficient of determination of $R^2 > 0.98$.

Statistical Analysis

Survival and qPCR data were analyzed using 1-way ANOVA. Values are expressed as means ± SEM of 3 independent observations unless indicated otherwise. Statistical significance was evaluated by using a paired Student's *t*-test. For mitochondria analyses and inhibitor (UO126, LY294002, BK-1361) and ELISA data, a 2-way ANOVA was performed, followed by Scheffé's post hoc test. Calculations were performed with the Winstat standard statistical software package.

Results

MMPs and ADAM8 Expression in GBM ± TMZ

Initially, a qPCR screen was performed in U87 cells to detect MMPs and ADAM genes induced under TMZ treatment for 5 days (Fig. 1A and B). Notably, mRNA levels of MMP-1, -9, -14, and ADAM8 were induced by TMZ after 5 days. These MMPs and ADAM8 are reported to be increased in glioblastomas,[16–18,28] but no data are available for recurrent GBM tissues from patients who underwent adjuvant therapy (TMZ,

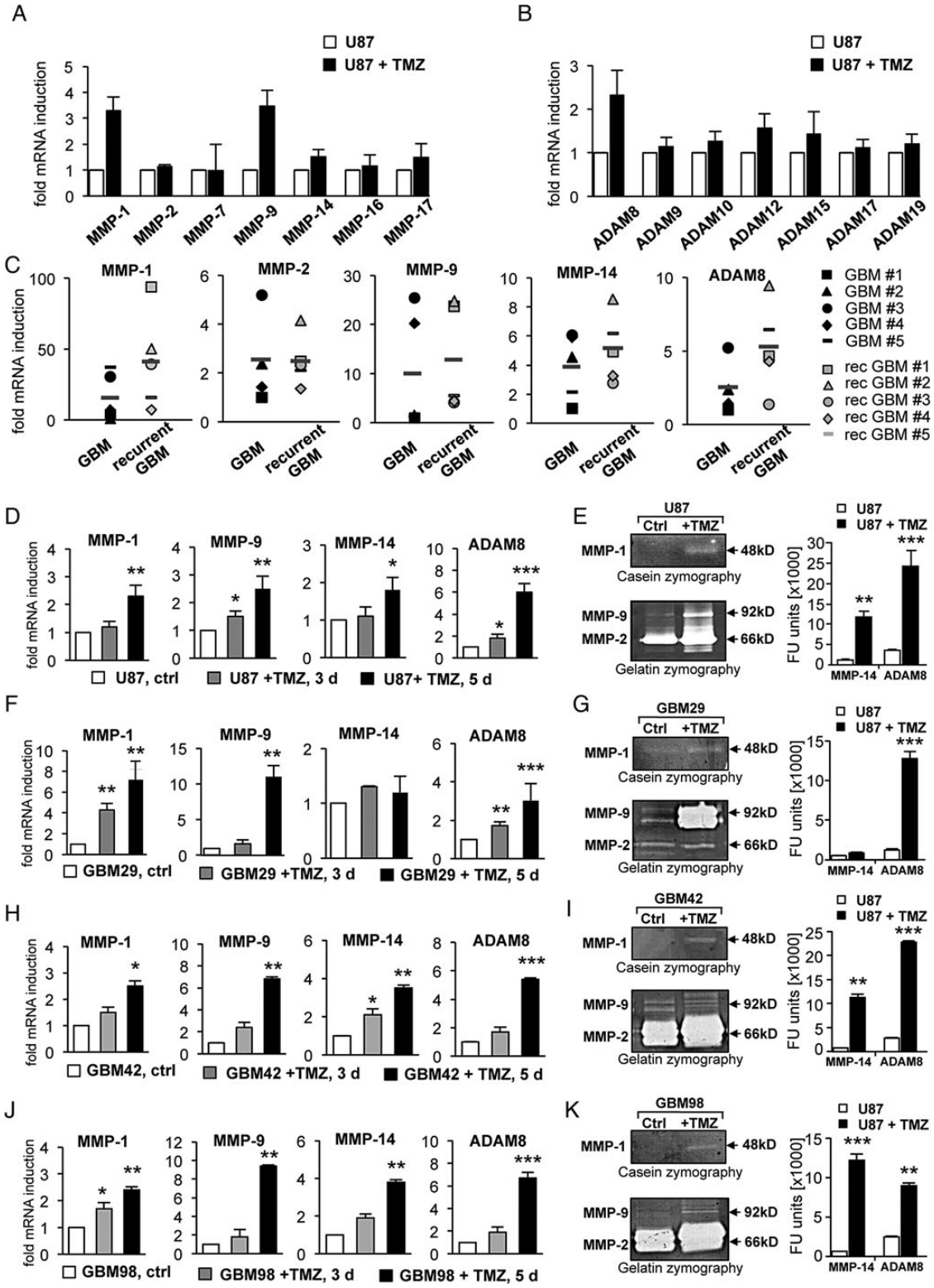

Fig. 1. MP expression in GBM cells, in GBM and recurrent GBM patient samples. Levels of mRNA of (A) MMPs and (B) ADAM proteases in U87 cells after treatment with 700 μM TMZ for 5 days. Relative expression determined by qPCR is presented as fold induction over untreated control. (C) MMP-1, -2, -9, -14, and ADAM8 in primary GBM compared with recurrent GBM patient samples. Values for individual patient samples (black and gray shapes). Mean values are shown by a horizontal line, derived from independent runs performed in triplicates and presented relative to the lowest expression value observed in the GBM patient cohort (=1). All samples for recurrent GBM were selected on the basis of a documented adjuvant TMZ therapy. (D) Analysis by qPCR to quantify mRNA levels of MMP-1, -9, -14, and ADAM8 by TMZ in U87, and 3 primary GBM

radiotherapy). Quantitative PCR was performed in tissues from 5 primary GBM and 5 recurrent GBM samples following adjuvant therapy with TMZ (Fig. 1C). MMP-1 mRNA levels were barely detectable in GBM samples (ΔCt values >30) but were induced in recurrent GBM (mean-fold induction over control: 15.9× for GBM, 41.2× for recurrent GBM). MMP-2 mRNA levels were unchanged in GBM versus recurrent GBM. MMP-9 mRNA was higher in recurrent GBM (10× for GBM; 12.5× for recurrent GBM). Moreover, MMP-14 mRNA was slightly higher in recurrent GBM (3.9× for GBM, 5.1× for recurrent GBM). ADAM8 expression was induced by TMZ, increasing from 2.5× for primary GBM to 5.3× for recurrent GBM. Given the similar MP induction profiles observed in TMZ-treated GBM cells and in recurrent GBM specimens, we hypothesize that expression of MMP-1, -9, -14, and ADAM8 in GBM cell lines could be mechanistically relevant for chemoresistance and invasive behavior of recurrent GBM cells.

Transcriptional induction of MMP-1, -9, -14, and ADAM8 by TMZ

To analyze TMZ-induced expression of MPs in GBM cells, qPCR was performed in U87 and 3 primary GBM cells—GBM29, GBM48, and GBM98—derived from tumor tissue of GBM WHO grade IV according to neuropathological classification (Fig. 1D, F, H, and J). Incubation with 700 μM TMZ for 3 days caused small differences in expression levels of MMPs/ADAMs. After 5 days, TMZ caused increased expression levels of MMP-9 and ADAM8 in all GBM cells, whereas MMP-14 was induced in all cells except GBM29. In U87 cells, ADAM8 expression levels were increased by 6× over control ($P<.01$). Expression levels of MMP-1, MMP-9, and MMP-14 were increased by 2.5×, 1.8×, and 1.7×, respectively (Fig. 1D). In GBM29 cells, MMP-1 levels were increased 7×, MMP-9 10.8×, and ADAM8 3× (Fig. 1F), whereas in primary GBM42 and GBM98, the strongest induction was seen for ADAM8 (Fig. 1H and J).

Protein expression of MMP-1, -9, -14, and ADAM8

Activity analyses of GBM cell supernatants were performed to confirm mRNA expression data. MMP-1, MMP-2, and MMP-9 were detected by casein and gelatin zymography, whereas MMP-14 and ADAM8 activities were determined by fluorescence assays using specific MMP-14 and ADAM8 substrates, respectively (Fig. 1E, G, I, and K). In U87 cells, MMP-1 was barely detectable by casein zymography as a 48-kD band, representing active MMP-1. MMP-2 and MMP-9 activities were detected by gelatin zymography (Fig. 1E) with strong MMP-2 (66 kD) activity in both samples (control vs TMZ treated) but no significant difference. In contrast, MMP-9 (92 kD) activity was significantly detectable in supernatants from TMZ-treated U87 cells (Fig. 1E). TMZ-induced MMP-14 and ADAM8 activities were detected by fluorescence assays. Similar results were obtained in supernatants from primary GBM cells (Fig. 1G, I, and K) and demonstrate that changes observed on mRNA levels for MMP-1, -9, -14, and ADAM8 reflect their biological activities. In contrast to all GBM cells investigated, U251 cells showed no significant activities of MMP-1, -9, and -14, whereas only a weak induction of ADAM8 activity by TMZ was observed (Supplementary Fig. 2B).

Dose- and time-dependent effect of TMZ on GBM cells

GBM cells were treated for 3 and 5 days with increasing concentrations of TMZ (50, 200, 700 μM; Fig. 2). To investigate whether the observed residual cell survival could be due to the presence of metalloprotease (MMP and ADAM) activities, GBM cells were subjected to cotreatment of TMZ plus BB-94, a broad-range MMP inhibitor.[39] In the presence of 700 μM TMZ and 100 nM BB-94 (see Supplementary Table 1 for half-maximal inhibitory concentration [IC_{50}] values), viabilities of GBM cells detected after 3 and 5 days were reduced by 50% compared with single TMZ treatment (Fig. 2A–D), suggesting that inhibition of MPs could contribute to TMZ sensitization of GBM cells from different tumor samples independently of their MGMT status.

ADAM8 Causes Chemoresistance of GBM Cells

In addition to BB-94, we used BB-2516 (marimastat, 200 nM) as an effective inhibitor of MMP-1, -9, and -14, but not of ADAM8 (Supplementary Table 1). All GBM cell specimens were subjected to TMZ treatment in the presence or absence of 200 nM BB-2516 (Fig. 3A). In contrast to BB-94, TMZ treatment with BB-2516 for 5 days did not cause sensitization of GBM cells (Fig. 3A), as cell survival rates in the absence or presence of BB-2516 were similar in all GBM cell specimens investigated. These data suggest that ADAM8 could be the major protease conferring TMZ chemoresistance to GBM cells. To investigate this hypothesis, U87 cells with high endogenous *ADAM8* expression (Supplementary Fig. 1) were used to generate stable *ADAM8* knockdown clones (U87_shA8), a scramble control (U87_shCtrl), and overexpressing cell clones (U87_A8) to analyze the effect of TMZ on variable *ADAM8* levels in a genetically homogeneous cell background (Fig. 3B). Cell survival assays were performed using U87 cell clones (Fig. 3C and D). In U87_shA8 cells treated with 50, 200, and 700 μM TMZ, cell viabilities were reduced by 50% after 3 days and by 60% after 5 days compared with control cells (Fig. 3C and D). Moreover, the number of surviving cells in ADAM8-overexpressing U87_A8 cells was significantly increased so that after 3 days (82% survivors) and 5 days (49% survivors) of treatment with 700 μM TMZ, up to 50% of cells survived, demonstrating that gene dosage of *ADAM8* in U87 cells has a significant effect on the observed TMZ chemoresistance of GBM cells. In cells with endogenous *ADAM8* expression levels, such as U251, TMZ desensitization was not observed (Supplementary Fig. 2C); however, in U251 cells generated to overexpress ADAM8 (U251_A8), cells were significantly more resistant to TMZ

cells: (F) GBM29, (H) GBM42, and (J) GBM98 after 3 and 5 days relative to control (=1) . Results represent 3 independent experiments performed in triplicate ($n=9$) and given as means ± SEM. Significance was calculated by Student's *t*-test with P *<.01, **<.005, ***<.001. Casein/gelatine zymography and fluorescence activity assays in (E) U87, (G) GBM29, (I) GBM42, and (K) GBM98 cell supernatants after TMZ treatment (700 μM, 5d) compared with untreated cells ("ctrl"). Fluorescence units (FU ×1000) were obtained after 3 h and given as means ± SEM. Significance was calculated by Student's *t*-test with P **<.005, ***<.001.

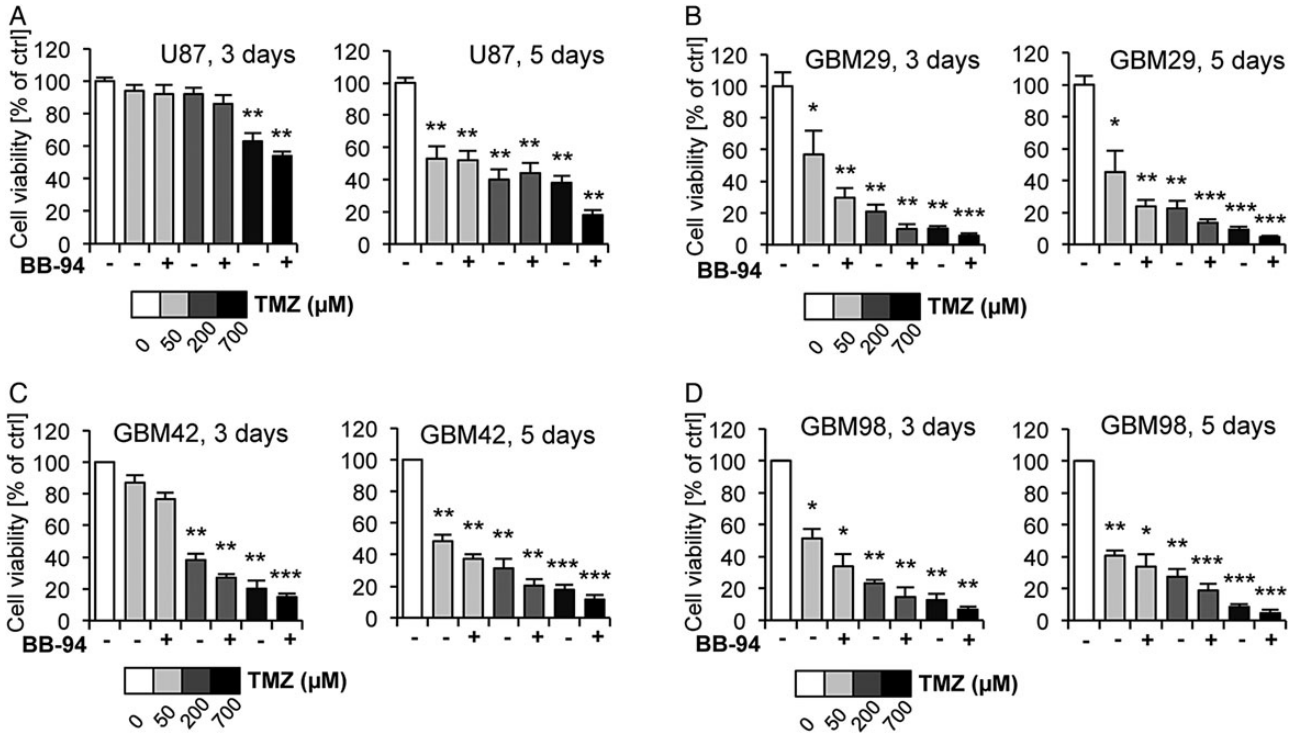

Fig. 2. Dose- and time-dependent effect of TMZ on GBM cells. (A) U87, (B) GBM29, (C) GBM42, and (D) GBM98 cells were analyzed for cell survival after 3 and 5 days following administration of 50, 200, and 700 μM TMZ (concentration indicated by grayscale code below diagrams), either alone or in combination with 100 nM BB-94 (batimastat) compared with control cells (vehicle only). After incubation times indicated, cells were fixed and stained with Hoechst dye, and numbers of surviving cells were counted under a fluorescence microscope. Cell counting was performed in 50 independent viewing fields and values are means ± SEM. Student's *t*-test was used for statistical significance; $^{*}P < .01$, $^{**}P < .001$, and $^{***}P < .0003$.

treatment. (Supplementary Fig. 2F). In addition, survival of GBM cells was analyzed in the presence of a pharmacological ADAM8 inhibitor, BK-1361[36] (Fig. 3E). ADAM8 inhibition causes sensitization to TMZ in GBM cells, arguing for a prominent role of ADAM8 in chemoresistance of GBM cells.

ADAM8 Affects Intracellular PI3K/Akt and ERK1/2 Signaling

To investigate the signaling mechanism of ADAM8-mediated chemoresistance, kinase activation was analyzed comparing U87_shCtrl with U87_shA8 cells by a kinase array kit (ARY003B, R&D Systems; see Supplementary Fig. 3). Phosphorylation of Akt (S473) was ~2.5× and of ERK1/2 ~1.3× lower in U87_shA8 cells. Western blots were performed to analyze TMZ-dependent activation of Akt and ERK1/2 (Fig. 4). In U87 cells, pAkt levels correlated with ADAM8 levels—that is, in U87_shA8 cells, pAkt levels were significantly lower than in U87_shCtrl cells. In both cell types, pAkt (S473) levels were not changed upon TMZ treatment in U87_shCtrl and in U87_shA8 cells. A strong increase in pAkt was observed in U87_A8 cells after 5 days treatment with 700 μM TMZ. Also for ERK1/2 phosphorylation, a correlation with *ADAM8* levels was observed, but the overall TMZ inducibility of pERK1/2 was not affected and strong in U87_A8 cells. Higher pAkt levels in either U87_shCtrl or U87_A8 cells could account for a positive effect of ADAM8 on cell survival. In contrast, low pAkt in U87_shA8 cells could be correlated to increased cell death. The effect of MPs on TMZ-dependent cell death was not due to mitochondrial effects, although TMZ caused significant changes in mitochondrial morphology and membrane potential (see Supplementary Fig. 4). For primary GBM cells, ERK1/2 activation was only affected by TMZ treatment in GBM29 cells. In contrast, GBM42 and GBM98 cells showed a higher degree of pAkt levels upon TMZ stimulation (Fig. 4E–H). These data suggest that ADAM8 causes chemoresistance via activation of pERK1/2 and/or pAkt.

ADAM8-mediated Signaling in GBM Invasion

Since ADAM8 has been linked to increased invasiveness of GBM cells,[40] we next investigated whether TMZ-mediated induction of MPs including ADAM8 causes increased invasion of TMZ-resistant GBM cells. Resistant vital GBM cells were treated with 700 μM TMZ for 5 days and were seeded on Matrigel invasion chambers (Fig. 5). For TMZ-treated U87 (Fig. 5A) and GBM cells (Fig. 5B–D), significant increases in the number of invaded cells were observed. However, in the presence of BB-94 (100 nM), BK-1361 (1 μM), U0126 (10 μM), and LY294002 (10 μM), invasion capacities of GBM cells were reduced to variable extents. In this assay the capacity of the kinase inhibitors U0126 and LY294002 to reduce TMZ-dependent invasion reflected the kinase activation profiles observed in GBM cells (Fig. 4). It is notable that BB-94 and BK-1361 reduced

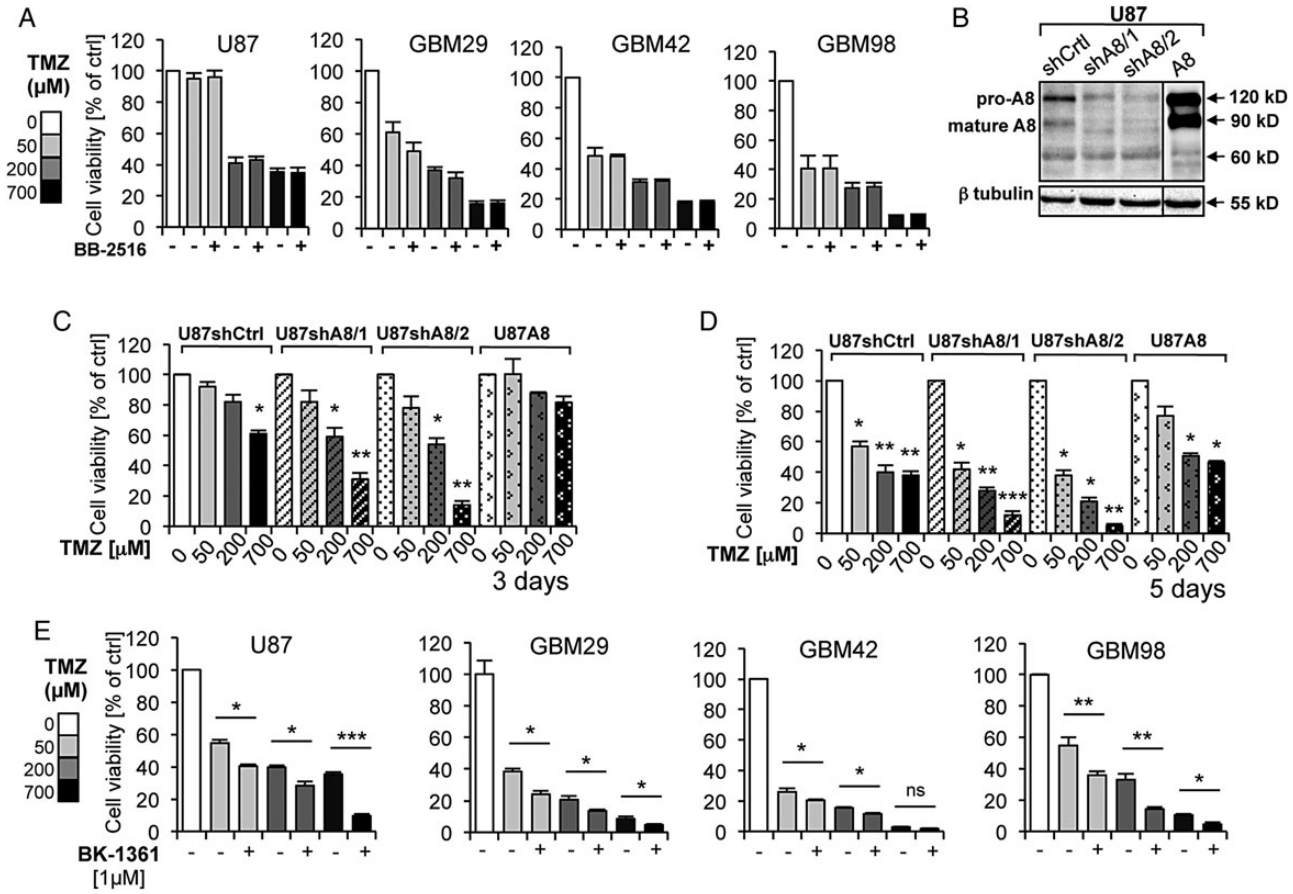

Fig. 3. ADAM8 causes resistance of GBM cells to TMZ. (A) Cell viability assays as shown in Fig. 2 were performed in U87, GBM29, GBM42, and GBM98 cells using 200 nM BB-2516 (marimastat), a concentration below the IC_{50} value for ADAM8 (Supplementary Table 1). Results are based on cell counts of 50 independent viewing fields in 3 independent experiments. Note that in contrast to BB-94, there is no significant difference in cell survival comparing BB-2516 treated with untreated cells. (B) Western blot for ADAM8 in 2 representative U87 knockdown clones (shA8) compared with a control scramble shRNA clone (shCtrl) and U87 cells overexpressing ADAM8 (U87_A8). Compared with U87_shCtrl cells, ADAM8 expression in U87_shA8 cell clones is reduced by >20-fold (see Supplementary Fig. 1). Cell viability in ADAM8 knockdown and ADAM8-overexpressing cells was determined as described in Fig. 2 after (C) 3 and (D) 5 days compared with U87_shCtrl cells. Values are presented as means ± SEM and significance was analyzed using Student's *t*-test with $^{*}P < .01$, $^{**}P < .001$. (E) Cell viability assay of U87, GBM29, GBM42, and GBM98 cells after 5 days TMZ treatment (50, 200, and 700 μM) in the presence of the specific ADAM8 inhibitor BK-1361 (1 μM). Results were obtained from 3 independent experiments performed in triplicate. Values are presented as means ± SEM. Statistical significance was analyzed using Student's *t*-test with $^{*}P < .02$, $^{**}P < .001$, $^{***}P < .0001$.

TMZ-induced invasiveness more significantly than did the kinase inhibitors, suggesting that MPs, in particular ADAM8, play a critical role in occurrence of invasive recurrent GBM cells.

Substrate Identification of TMZ-treated GBM Cells

To analyze potential substrates of ADAM8 conferring the observed invasiveness of GBM cells, a proteomic analysis using CCM from U87 cells was performed. Since cell invasion critically depends on extracellular shedding activities, we were particularly interested in proteins annotated to the cell surface—for instance, due to the presence of a transmembrane domain or a glycosylphosphatidylinositol anchor. Stable isotope tagging was used to unravel changes in the proteome composition of CCM from U87 cells (700 μM TMZ vs 700 μM TMZ/100 nM BB-94). We based our analysis on the ASAPratio platform[38] and chose a *P*-value cutoff <.05 to discern significant proteomic alterations. From 899 proteins analyzed in total, 14 cell surface proteins were affected (Table 1). In all cases, a decrease in relative protein abundance was found as expected when inhibiting cell surface shedding. Similarly, in all of these cases the identified peptides originated from putatively shed ectodomains. These results emphasize that BB-94 affects cell surface proteolysis. For CD44 and HGF R/c-met, a lower abundance in supernatants from TMZ/BB-94–treated cells was detected (Table 1). The presence of soluble CD44 and soluble HGF R/c-met due to proteolytic release of their ectodomains was confirmed by ELISA (Fig. 5E). Higher levels of soluble CD44 and soluble HGF R/c-met were found in TMZ-treated U87 cells, whereas significantly lower levels were found in U87 cells cotreated with BB-94 or in U87_shA8 knockdown cells. These results suggest that at least in part, ADAM8 could be

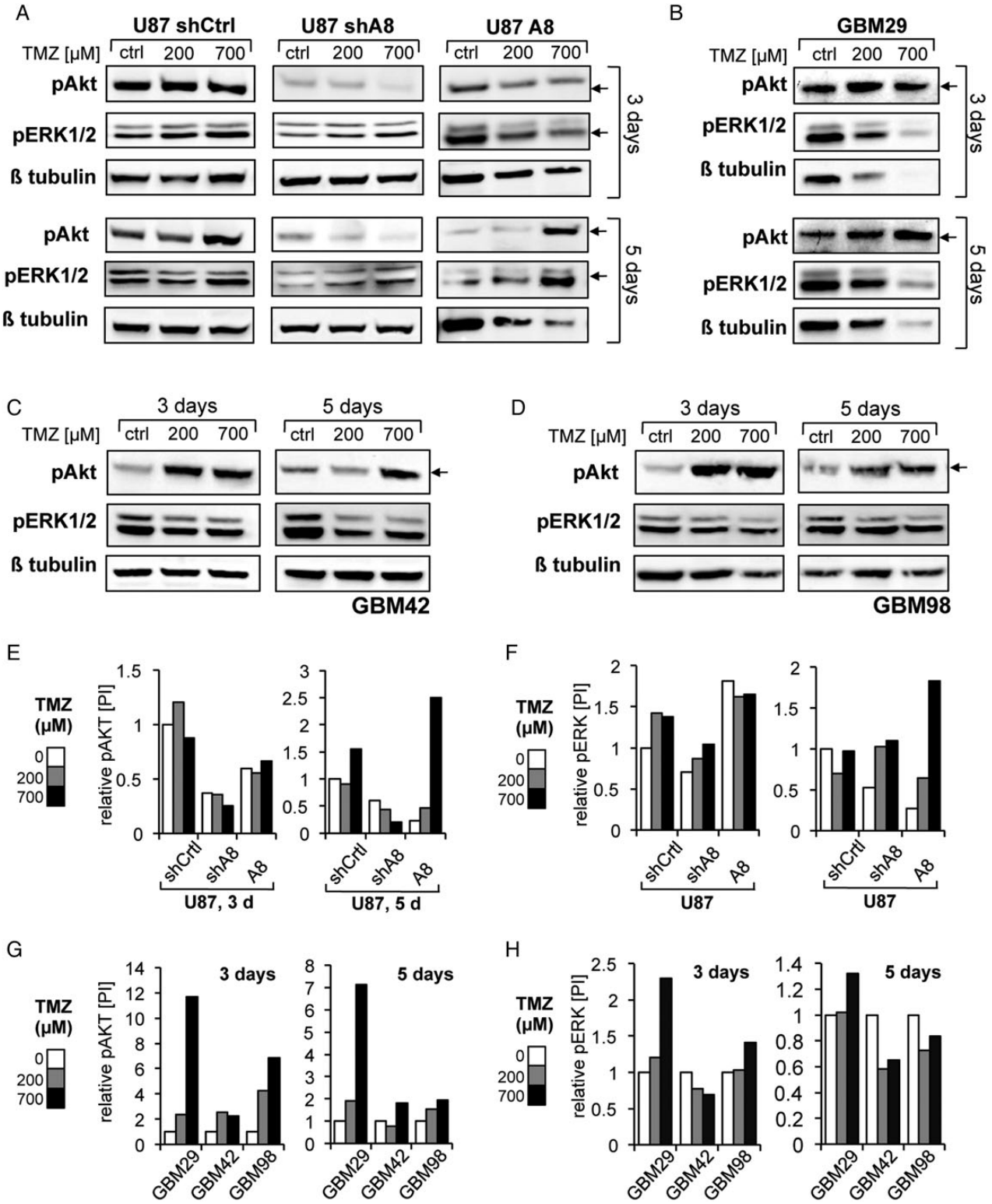

Fig. 4. Kinase signaling in U87 cells with different ADAM8 levels. U87_shCtrl, U87_shA8, U87_A8, GBM29, GBM42, and GBM98 cells were treated with 200 and 700 μM TMZ for 3 and 5 days, respectively. Cell lysates were subjected to western blot analysis. Levels of pERK1/2 (Tyr 202/204) and pAkt (S473) were detected using specific antibodies. Changes in kinase phosphorylation are indicated by arrows. Note that pAkt and pERK1/2 levels are significantly lower in U87_shA8 cells compared with control and, after TMZ induction, significantly higher in U87_A8 cells after 5 days. Quantification of western blot signals was performed for (F and H) pERK1/2 and (E and G) pAkt in all GBM cells analyzed by using ImageJ software (National Institutes of Health) and are presented relative to untreated cell samples (=1).

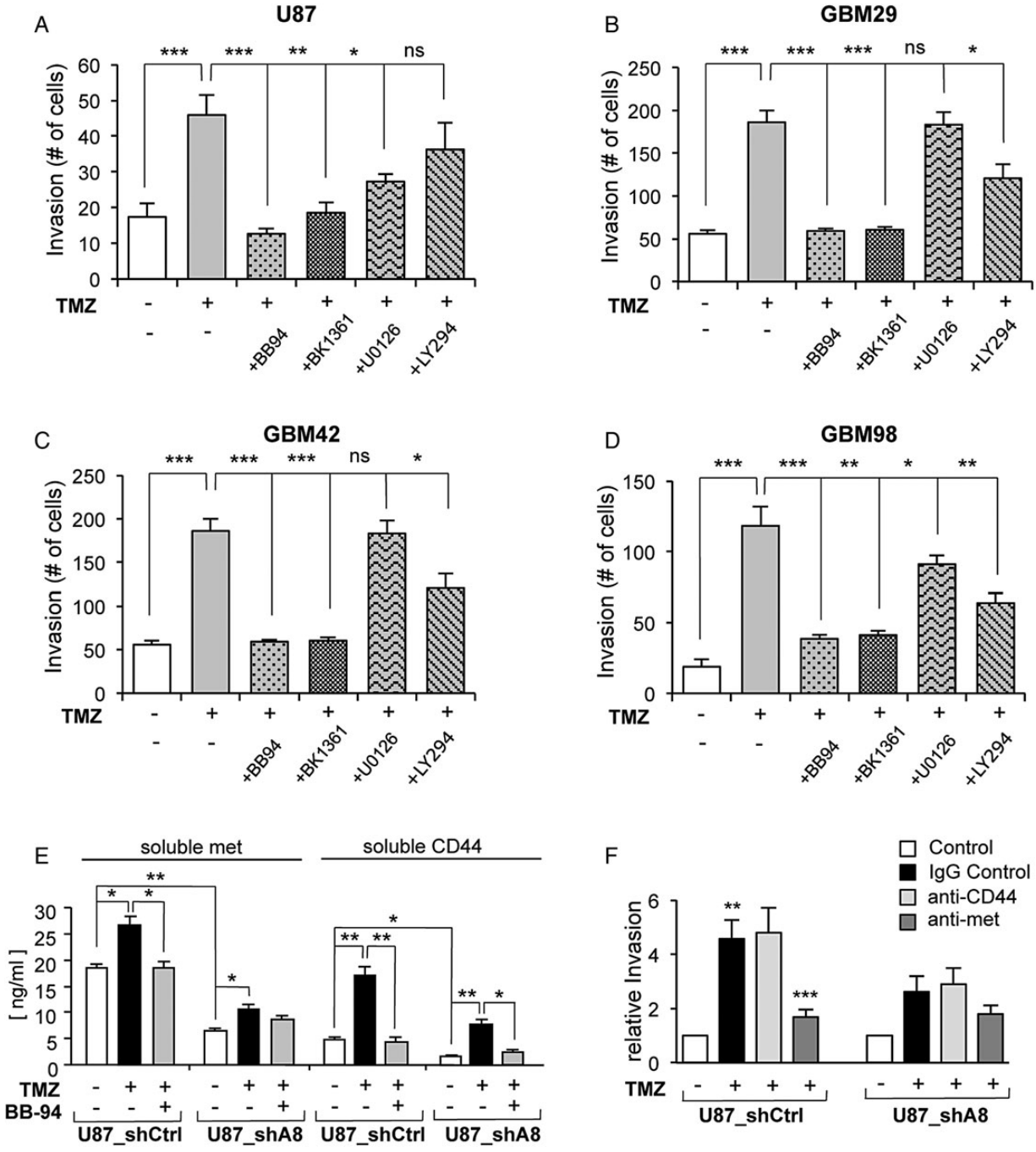

Fig. 5. Role of ADAM8 for TMZ-induced invasion of GBM cells. TMZ-induced invasion in GBM cells (A) U87, (B) GBM29, (C) GBM42, and (D) GBM98. Five days after addition of TMZ to GBM cells, relative differences in invasiveness were analyzed by Matrigel invasion assays. Compared with control GBM cells (white bars), TMZ-induced invasiveness (gray bars) observed for all GBM cells is dependent on metalloprotease activity, as BB-94 (100 nM, spotted gray bar) reduced TMZ-induced invasiveness to basal levels. A similar effect was observed for the ADAM8 inhibitor BK-1361 (dark gray bar); in contrast, inhibiton neither of ERK1/2 by U0126 nor of PI3K/Akt by LY294002 (hatched gray bars) had a comparable effect on TMZ-induced GBM invasion. Values are means ± SD of 3 independent experiments performed in triplicate. Statistical significances were calculated by Student's *t*-test with $^{*}P < .01$, $^{**}P < .005$, $^{***}P < .001$. (E) Soluble protein levels of potential ADAM8 substrates (see Table 1) c-met (HGF receptor) and CD44 (hyaluronic acid receptor) as determined by ELISA in supernatants from U87_shCtrl and U87_shA8 cells 5 days after TMZ addition. Identical protein concentrations were used for ELISA; values are calculated based on standard curves and given as means ± SEM of at least 3 replicates. Student's *t*-test was performed to evaluate statistical significance; $^{*}P < .005$, $^{**}P < .001$. (G) Blocking antibodies (10 μg/mL) directed against CD44 and HGF R/c-met were used for invasion assays performed with either U87_shCtrl or U87_shA8 cells. An irrelevant IgG was used as control antibody. Cell invasion was determined by calcein acetoxymethyl fluorescence measurement in 3 independent samples. Values are given as relative changes over control conditions (=1) for U87_Ctrl and U87_shA8.

Table 1. Significantly affected proteins by BB-94 treatment

Uniprot	*P*-value	Fc-value	SD	Name
CD166_HUMAN	1.89E-05	−2.26	0.22	CD166 antigen
CAH9_HUMAN	2.97E-02	−2.45	1.78	Carbonic anhydrase 9
CD276_HUMAN	1.75E-04	−2.00	0.22	CD276 antigen
CD44_HUMAN	3.60E-04	−1.83	0.08	CD44 antigen
CD59_HUMAN	4.86E-02	−1.15	0.25	CD59 glycoprotein
1B07_HUMAN	3.34E-05	−2.41	0.48	Human leukocyte antigen class I histocompatibility antigen, B-7 alpha chain
ITA5_HUMAN	6.01E-03	−1.46	0.18	Integrin alpha-5
LMAN2_HUMAN	6.01E-03	−1.05	0.07	Vesicular integral-membrane protein VIP36
MET_HUMAN	1.94E-02	−1.32	0.25	Hepatocyte growth factor receptor
NTNG1_HUMAN	2.41E-03	−1.66	0.24	Netrin-G1
EPCR_HUMAN	2.74E-05	−2.68	0.74	Endothelial protein C receptor
THY1_HUMAN	1.49E-02	−1.29	0.15	Thy-1 membrane glycoprotein
VASN_HUMAN	2.27E-02	−1.16	0.06	Vasorin

Due to the focus on cell surface proteolysis, only cell surface proteins (transmembrane domain or glycosylphosphatidylinositol anchor) are listed. Uniprot ID and recommended name according to Uniprot database (Uniprot Consortium, 2013). *P*-value denotes the significance of a protein being quantitatively affected. *P*-values, Fc-values (log_2 of light:heavy ratio), and corresponding SD were calculated by ASAPratio.[38]

involved in the proteolytic release of CD44 and HGF R/c-met from U87 cells. To analyze the functional role of these proteins for TMZ-induced invasiveness, as observed in recurrent GBM, we performed invasion assays 5 days after induction of U87_shCtrl and U87_shA8 cells with 700 μM TMZ and analyzed the mechanistic role of CD44 and HGF R/c-met by blocking antibodies against these proteins (Fig. 5F). In U87_shA8 cells, invasiveness is low and can be slightly induced by TMZ (2.4×). Using anti-CD44 had no effect on invasion, whereas a blocking antibody against c-met had a slight, although not significant, effect. In contrast, U87_shCtrl cells were significantly induced in their invasiveness by TMZ. Whereas an anti-CD44 blocking antibody had no effect, an HGF R/c-met antibody reduced TMZ-induced invasiveness to nearly control level (Fig. 5F). Thus we demonstrated that an increase in ADAM8 levels correlates with c-met levels, which both might have a functional role in TMZ-induced invasiveness.

Discussion

The efficacy of TMZ as the gold standard for treatment of malignant glioma[3] is limited by acquired resistance of glioma cells,[4,9,10] which underpins the need to understand the molecular mechanisms of chemoresistance. MGMT expression determines TMZ resistance in patients, as shown by efficacy studies in patients with methylated or unmethylated MGMT promoter. To account for this, GBM cells with methylated MGMT promoter (U87, U251, and GBM29) and unmethylated MGMT promoter status (GBM42 and GBM98) were included in our study. The observed differences in cell survival comparing all GBM cells suggest mechanisms of TMZ resistance in addition to MGMT. Since U87 cells were by far the most resistant cells in vitro,[41] this cell line is suitable to identify resistance mechanisms. Earlier studies demonstrated that MMPs are involved in TMZ resistance of GBM cells,[42,43] and the effect of BB-94 on glioma growth was discussed extensively.[19] Severe side effects of BB-94 ruled out cotherapy of TMZ and BB-94. Alternatively, the less toxic marimastat (BB-2516) was used in clinical studies treating GBM patients with either TMZ + BB-2516 or TMZ alone.[23] As a result, no significant effect on GBM patient survival was observed, strongly suggesting that BB-2516–insensitive MMPs or ADAMs contribute to chemoresistance in GBM. By qPCR analysis of TMZ-inducible MMPs and ADAM proteases in GBM cells, ADAM8 and MMP-1, -9, and -14 were identified as potential modulators of chemoresistance in GBM cells. In all GBM cell lines investigated, BB-94 sensitized GBM cells to TMZ treatment within 3–5 days after addition of TMZ, in accordance with dose-dependent apoptosis in GBM cells at time points starting after 72–96 h.[44] In combination with TMZ, BB-94 was used in concentrations of 100 nM, well above the IC_{50} values for MMPs and ADAM8. At 100 nM, BB-94 itself had no effect on cell proliferation, as demonstrated earlier for concentrations at or above 10 μM.[19]

Comparing the 2 experimental groups (TMZ vs TMZ + BB-94), significant differences in viability of ∼20% were shown for GBM cells. These differences in viabilities were not observed with marimastat (TMZ vs TMZ + BB-2516). Of the 4 MPs induced by TMZ, ADAM8 is the only protease not inhibited by BB-2516 (IC_{50} ∼1.2 μM with recombinant ADAM8). Thus, the observed differences in viabilities between BB-94 (100 nM) and BB-2516 (100 nM) might be due to TMZ-induced expression of ADAM8. Interestingly, the expression levels of ADAM8 in primary GBM cells were comparable to endogenous ADAM8 levels of U87 cells, so that this cell line might reflect the pathological situation in GBM. Even in GBM cells with low ADAM8 expression, such as U251, TMZ inducibility could be observed. ADAM8 regulates TMZ sensitivity in a dose-dependent manner: a 20% higher degree of cell death in ADAM8 knockdown cells was observed and reflected the effect caused by BB-94. Higher ADAM8 expression caused increased resistance in U87_A8 cells. Thus, our results suggest that ADAM8 expression levels can affect TMZ resistance of GBM cells.

Mechanistically ADAM8-dependent differences were observed in pAkt and pERK1/2 levels, which could account for cell survival and invasiveness, respectively. We found reduced pAkt levels in U87_shA8 cells that were not inducible even by high TMZ concentrations (700 μM) or by longer incubation times (5 d). In contrast, overexpression of ADAM8 leads to increased pAkt and pERK1/2 levels with 700 μM TMZ. In primary GBM cells, the Akt/PI3K pathway is more prominent than the pERK pathway and has been described with regard to dysregulation in GBM[45] and therapy resistance.[46] In this respect, regulation of ATP-binding cassette transporters such as ABCG2 by pAkt could be instrumental in the observed TMZ resistance.[47]

In addition to chemoresistance, MMPs and ADAM8 regulated by TMZ contribute to enhanced invasiveness. Since U0126 in U87 and LY294002 in GBM cells reduced TMZ-induced invasiveness, pERK1/2 or pAkt is able to mediate TMZ-induced invasiveness of GBM cells.

Proteomics comparing U87 cells (TMZ vs TMZ + BB-94) allowed identification of CD44 and c-met as substrates of MPs induced by TMZ. CD44 (hyaluronic acid receptor) and c-met (HGF receptor) are crucial for glioma migration and invasiveness.[29,30] TMZ-induced CD44 and c-met shedding could be instrumental for increased invasiveness of GBM cells under therapy and might have an impact on formation of recurrent GBM via activation of GBM stem cells through c-met.[40]

Our results identified ADAM8 as a protease involved in TMZ-induced chemoresistance and enhanced invasion of GBM cells by modulating pERK1/2 and pAkt pathways and by shedding of invasion-relevant substrates CD44 and c-met. Thus, specific inhibition of ADAM8 in future therapy regimens could optimize TMZ chemotherapy and prevent formation of recurrent GBM.

Supplementary Material

Supplementary material is available online at *Neuro-Oncology* (http://neuro-oncology.oxfordjournals.org/).

Funding

Funding was provided by Cancer Research Technology, London (J.W.B.), Tongji Medical Hospital (F.D.), and Stiftung Tumorforschung Kopf-Hals (H.S.). O.S. was funded by Deutsche Forschungsgemeinschaft (SCHI 871/2, SCHI 871/5, and SFB 850 project B8), by a starting grant from the European Research Council (programme "Ideas"; call identifier: ERC-2011-StG 282111-ProteaSys), and the Excellence Initiative of the German Federal and State Governments (EXC 294, BIOSS).

Acknowledgments

The authors thank Sabine Motzny, Bettina Mayer, and Franz Jehle for excellent technical assistance, Sabrina Donges for analysis of MGMT status, Vincent Dive and Fabrice Beau (Gif sur Yvette, France) for the kind gift of MT1-MMP substrate, and Prof Ting Lei, Department of Neurosurgery, Tongji Medical Hospital, Wuhan, for continuous support.

Conflict of interest statement. The authors declare no conflicts of interest.

References

1. Louis DN, Ohgaki H, Wiestler OD, et al. The 2007 WHO classification of tumours of the central nervous system. *Acta Neuropathol*. 2007;114(2):97–109.
2. Giese A, Westphal M. Glioma invasion in the central nervous system. *Neurosurgery*. 1996;39(2):235–250; discussion 250–232.
3. Stupp R, Mason WP, van den Bent MJ, et al. Radiotherapy plus concomitant and adjuvant temozolomide for glioblastoma. *N Engl J Med*. 2005;352(10):987–996.
4. Strik HM, Marosi C, Kaina B, et al. Temozolomide dosing regimens for glioma patients. *Curr Neurol Neurosci Rep*. 2012;12(3):286–293.
5. Baker SD, Wirth M, Statkevich P, et al. Absorption, metabolism, and excretion of 14C-temozolomide following oral administration to patients with advanced cancer. *Clin Cancer Res*. 1999;5(2):309–317.
6. Villano JL, Seery TE, Bressler LR. Temozolomide in malignant gliomas: current use and future targets. *Cancer Chemother Pharmacol*. 2009;64(4):647–655.
7. Beier D, Schulz JB, Beier CP. Chemoresistance of glioblastoma cancer stem cells—much more complex than expected. *Mol Cancer*. 2011;10:128.
8. Roos WP, Kaina B. DNA damage-induced cell death by apoptosis. *Trends Mol Med*. 2006;12(9):440–450.
9. Kitange GJ, Carlson BL, Schroeder MA, et al. Induction of MGMT expression is associated with temozolomide resistance in glioblastoma xenografts. *Neuro Oncol*. 2009;11(3):281–291.
10. Ulasov IV, Nandi S, Dey M, et al. Inhibition of sonic hedgehog and Notch pathways enhances sensitivity of CD133(+) glioma stem cells to temozolomide therapy. *Mol Med*. 2011;17(1–2):103–112.
11. Cheng L, Wu Q, Huang Z, et al. L1CAM regulates DNA damage checkpoint response of glioblastoma stem cells through NBS1. *EMBO J*. 2011;30(5):800–813.
12. Riedle S, Kiefel H, Gast D, et al. Nuclear translocation and signalling of L1-CAM in human carcinoma cells requires ADAM10 and presenilin/gamma-secretase activity. *Biochem J*. 2009;420(3):391–402.
13. Moss ML, Bartsch JW. Therapeutic benefits from targeting of ADAM family members. *Biochemistry*. 2004;43(23):7227–7235.
14. Boire A, Covic L, Agarwal A, et al. PAR1 is a matrix metalloprotease-1 receptor that promotes invasion and tumorigenesis of breast cancer cells. *Cell*. 2005;120(3):303–313.
15. Littlepage LE, Sternlicht MD, Rougier N, et al. Matrix metalloproteinases contribute distinct roles in neuroendocrine prostate carcinogenesis, metastasis, and angiogenesis progression. *Cancer Res*. 2010;70(6):2224–2234.
16. Forsyth PA, Laing TD, Gibson AW, et al. High levels of gelatinase-B and active gelatinase-A in metastatic glioblastoma. *J Neurooncol*. 1998;36(1):21–29.
17. Hur JH, Park MJ, Park IC, et al. Matrix metalloproteinases in human gliomas: activation of matrix metalloproteinase-2 (MMP-2) may be correlated with membrane-type-1 matrix metalloproteinase (MT1-MMP) expression. *J Korean Med Sci*. 2000;15(3):309–314.
18. Stojic J, Hagemann C, Haas S, et al. Expression of matrix metalloproteinases MMP-1, MMP-11 and MMP-19 is correlated with the WHO-grading of human malignant gliomas. *Neurosci Res*. 2008;60(1):40–49.
19. Tonn JC, Kerkau S, Hanke A, et al. Effect of synthetic matrix-metalloproteinase inhibitors on invasive capacity and

proliferation of human malignant gliomas in vitro. *Int J Cancer*. 1999;80(5):764–772.

20. Kargiotis O, Chetty C, Gondi CS, et al. Adenovirus-mediated transfer of siRNA against MMP-2 mRNA results in impaired invasion and tumor-induced angiogenesis, induces apoptosis in vitro and inhibits tumor growth in vivo in glioblastoma. *Oncogene*. 2008;27(35):4830–4840.
21. Nakada M, Okada Y, Yamashita J. The role of matrix metalloproteinases in glioma invasion. *Front Biosci*. 2003;8:e261–e269.
22. Badiga AV, Chetty C, Kesanakurti D, et al. MMP-2 siRNA inhibits radiation-enhanced invasiveness in glioma cells. *PLoS One*. 2011;6(6):e20614.
23. Groves MD, Puduvalli VK, Conrad CA, et al. Phase II trial of temozolomide plus marimastat for recurrent anaplastic gliomas: a relationship among efficacy, joint toxicity and anticonvulsant status. *J Neurooncol*. 2006;80(1):83–90.
24. Duffy MJ, Mullooly M, O'Donovan N, et al. The ADAMs family of proteases: new biomarkers and therapeutic targets for cancer? *Clin Proteomics*. 2011;8(1):9.
25. Edwards DR, Handsley MM, Pennington CJ. The ADAM metalloproteinases. *Mol Aspects Med*. 2008;29(5):258–289.
26. Blobel CP. ADAMs: key components in EGFR signalling and development. *Nat Rev Mol Cell Biol*. 2005;6(1):32–43.
27. Murphy G. The ADAMs: signalling scissors in the tumour microenvironment. *Nat Rev Cancer*. 2008;8(12):929–941.
28. Wildeboer D, Naus S, Amy Sang QX, et al. Metalloproteinase disintegrins ADAM8 and ADAM19 are highly regulated in human primary brain tumors and their expression levels and activities are associated with invasiveness. *J Neuropathol Exp Neurol*. 2006;65(5):516–527.
29. Ariza A, López D, Mate JL, et al. Role of CD44 in the invasiveness of glioblastoma multiforme and the noninvasiveness of meningioma: an immunohistochemistry study. *Hum Pathol*. 1995;26(10):1144–1147.
30. Koochekpour S, Jeffers M, Rulong S, et al. Met and hepatocyte growth factor/scatter factor expression in human gliomas. *Cancer Res*. 1997;57(23):5391–5398.
31. Lo HW. EGFR-targeted therapy in malignant glioma: novel aspects and mechanisms of drug resistance. *Curr Mol Pharmacol*. 2010;3(1):37–52.
32. Nakada M, Kita D, Teng L, et al. Receptor tyrosine kinases: principles and functions in glioma invasion. *Adv Exp Med Biol*. 2013;986:143–170.
33. He S, Ding L, Cao Y, et al. Overexpression of a disintegrin and metalloprotease 8 in human gliomas is implicated in tumor progression and prognosis. *Med Oncol*. 2012;29(3):2032–2037.
34. Zheng X, Jiang F, Katakowski M, et al. ADAM17 promotes glioma cell malignant phenotype. *Mol Carcinog*. 2012;51(2):150–164.
35. Zhang W, Wan M, Ma L, et al. Protective effects of ADAM8 against cisplatin-mediated apoptosis in non-small-cell lung cancer. *Cell Biol Int*. 2013;37(1):47–53.
36. Schlomann U, Koller G, Conrad C, et al. A critical role for ADAM8 in pancreatic cancer. *Nat Comm*. 2015;6:1–16.
37. Livak KJ, Schmittgen TD. Analysis of relative gene expression data using real-time quantitative PCR and the 2(-delta delta C(t)) Method. *Methods*. 2001;25(4):402–408.
38. Li XJ, Zhang H, Ranish JA, et al. Automated statistical analysis of protein abundance ratios from data generated by stable-isotope dilution and tandem mass spectrometry. *Anal Chem*. 2003;75(23):6648–6657.
39. Davies B, Brown PD, East N, et al. A synthetic matrix metalloproteinase inhibitor decreases tumor burden and prolongs survival of mice bearing human ovarian carcinoma xenografts. *Cancer Res*. 1993;53(9):2087–2091.
40. Joo KM, Jin J, Kim E, et al. MET signaling regulates glioblastoma stem cells. *Cancer Res*. 2012;72(15):3828–3838.
41. Johannessen TC, Prestegarden L, Grudic A, et al. The DNA repair protein ALKBH2 mediates temozolomide resistance in human glioblastoma cells. *Neuro Oncol*. 2013;15(3):269–278.
42. Gabelloni P, Da Pozzo E, Bendinelli S, et al. Inhibition of metalloproteinases derived from tumours: new insights in the treatment of human glioblastoma. *Neuroscience*. 2010;168(2):514–522.
43. Trog D, Yeghiazaryan K, Fountoulakis M, et al. Pro-invasive gene regulating effect of irradiation and combined temozolomide-radiation treatment on surviving human malignant glioma cells. *Eur J Pharmacol*. 2006;542(1–3):8–15.
44. Roos WP, Batista LF, Naumann SC, et al. Apoptosis in malignant glioma cells triggered by the temozolomide-induced DNA lesion O6-methylguanine. *Oncogene*. 2007;26(2):186–197.
45. Narayan RS, Fedrigo CA, Stalpers LJ, et al. Targeting the Akt-pathway to improve radiosensitivity in glioblastoma. *Curr Pharm Des*. 2013;19(5):951–957.
46. Falasca M. PI3 K/Akt signalling pathway specific inhibitors: a novel strategy to sensitize cancer cells to anti-cancer drugs. *Curr Pharm Des*. 2010;16(12):1410–1416.
47. Hou H, Sun H, Lu P, et al. Tunicamycin potentiates cisplatin anticancer efficacy through the DPAGT1/Akt/ABCG2 pathway in mouse xenograft models of human hepatocellular carcinoma. *Mol Cancer Ther*. 2013;12(12):2874–2884.